Structure and Temperature-Dependent Properties of Poly(4-methyl-1-pentene) Fibers

Srinath Reddy,[†] Prashant Desai,[‡] and A. S. Abhiraman*

Polymer Education and Research Center, Georgia Institute of Technology, Atlanta, Georgia 30332

Haskell W. Beckham,[§] Andrzej S. Kulik, and Hans W. Spiess

Max-Planck-Institut für Polymerforschung, Postfach 3148, D-55128 Mainz, Germany

Received July 30, 1996; Revised Manuscript Received January 17, 1997[⊗]

ABSTRACT: The origin of a dramatic loss of tensile strength in poly(4-methyl-1-pentene) [PMP] above a major dynamic mechanical transition that occurs around 45 °C is explored. The usual mechanisms associated with loss of strength in polymers are shown to be absent in this case. Viscous dissipation disappears almost completely during deformation of PMP above the transition of interest here. A thermodynamic analysis of reversible deformation is shown to provide remarkably good predictions of the work of rupture under such conditions. The thermorheological responses of PMP suggest that the transition of concern here is not accompanied by the onset of rapid backbone motions but by pendant group motions. Indeed, 2D wideline separation (WISE) NMR, which correlates dynamics (via ^{1}H widelines) with structure (via ^{13}C chemical shifts), clearly reveals that this transition is primarily accompanied by the onset of rapid pendant group motions. Such motions, coupled with the relatively large inter-backbone distances in PMP, provide the conditions necessary for elimination of viscous dissipation. These findings require refinement of the previously held view that the transition around 45 °C in PMP denotes a glass transition associated with the onset of rapid backbone segmental motions.

Introduction

Stereoregular poly(4-methyl-1-pentene) [PMP], as produced commercially, is a copolymer with 95+% head-to-tail, isotactic sequences of 4-methyl-1-pentene:

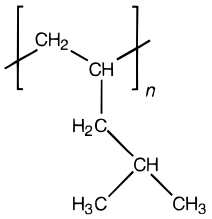

PMP has a low dielectric constant (2.12 at 25 °C and 10^2-10^4 Hz) and loss (dissipation factor at 10 MHz = 1.5×10^{-4}) and also a very low bulk density (∼0.83 g/cm^3).[1] The dielectric constant is the lowest among all synthetic resins that are reported in the literature. Its crystalline and amorphous densities are very close to each other,[2] giving a high degree of optical transparency to the material produced over a broad range of processing conditions. In fact, at room temperature the crystalline phase is slightly less dense than that of the amorphous phase, a manifestation of the helical conformation[3,4] in which the bulky isobutyl groups provide for a rather spacious crystalline unit cell.[2] Crystalline PMP has a melting temperature, T_m, of ∼245 °C, and a reported glass transition, T_g, of ∼45 °C.[5]

PMP has potentially a wide range of applications, owing to its optical and electrical properties, low bulk density, high chemical resistance, and high permeability to gases.[6] Its mechanical properties are comparable to other polyolefins at room temperature, with a melting temperature that is higher than that of the common polyolefins, polyethylene and polypropylene. These intrinsically desirable characteristics have led to several studies of the structure and properties of this polymer. These have been described in a comprehensive review by Lopez et al.[5] However, a major impediment to broad applications of this material is the significant deterioration of mechanical properties when the temperature is raised above room temperature, still well below its melting temperature. The tensile strength of PMP can decrease by as much as 90% when the temperature is increased from 25 to 80 °C.[7,8]

A number of dynamic mechanical studies as a function of temperature have been conducted.[9−12] In the region of room temperature to 200 °C, there is general agreement that at least two major transitions exist in PMP: one at 20−50 °C and another at 105−135 °C. Both transitions also appear in dilatometry data,[2] refractive index vs temperature curves, and thermally stimulated current spectra.[13] Each of these transitions is accompanied by a drop in shear modulus by a factor of 5. For comparison, the dynamic mechanical α transition of poly(1-butene) is accompanied by a factor-of-15 drop in shear modulus and identified as the glass transition.[12] The sharper transition in PMP at about 45 °C is typically defined as the glass transition. The significantly broader transition at about 130 °C has been associated with the onset of motions within the crystalline regions. X-ray diffraction studies as a function of temperature reveal a more rapid lattice expansion (*a* parameter of the unit cell) beginning at 125 °C.[14,15] On the other hand, dilatometric data showed that the 130 °C transition was much more evident in the completely amorphous polymer compared to the crystalline polymer.[2] Oftentimes the peaks in the dynamic mechanical loss factor curves contain shoulders; some researchers have labeled the shoulders and thereby identified four transitions in this temperature range.[11]

* To whom all communications should be addressed. School of Chemical Engineering, Georgia Institute of Technology.
[†] Present address: Alcatel Telecommunications, Roanoke, VA.
[‡] School of Textile & Fiber Engineering, Georgia Institute of Technology.
[§] Present address: School of Textile & Fiber Engineering, Georgia Institute of Technology.
[⊗] Abstract published in *Advance ACS Abstracts,* April 15, 1997.

S0024-9297(96)01139-4 CCC: $14.00

Thus, the complex thermorheological spectrum of this polymer is still largely unexplained. Since many applications may involve at least moderately elevated temperatures under an anisotropic stress field, there is a need to further characterize the nature and identify the cause of changes in the mechanical behavior of PMP as a function of temperature. We report here the results of an extensive investigation that eliminates conventional mechanisms for loss of strength in polymers as the underlying cause of the dramatic temperature-dependent decline of tensile properties in PMP. The real mechanism is then identified phenomenologically through the application of the results of a simple thermodynamic analysis that shows a quantitative correspondence to the experimental results. Solid-state NMR is used to connect the macroscopic observations with the molecular motions responsible for such observations.

Experimental Details

Two PMP filament bundles, one as-extruded (or "as-spun") and the other drawn at ~110 °C to a draw ratio of 1.5, were obtained from the research laboratories of Phillips Petroleum Co. Each bundle consisted of 100 filaments, with the linear densities of as-spun and drawn bundles being 236 and 157 dTex (g/10 000 m length of fiber bundle), respectively. Annealing studies on the fibers were performed in an air-circulating oven preheated to ~100 °C. For free length annealing (FLA), fibers were freely hung from a metal frame. For constant length annealing (CLA), the fibers were mounted on the frame taut with a minimum tension. This frame was introduced into the oven and removed after 2 min.

Differential scanning calorimetry was conducted using a Perkin-Elmer DSC-7 in a nitrogen atmosphere at 20 °C/min. The crystallinity of PMP was obtained from the ratio $\Delta H/\Delta H_c$, where ΔH = measured heat of fusion of the sample and ΔH_c = heat of fusion of the fully crystalline material, 61.7 J/g.[16]

Birefringence was obtained by measuring the refractive indices with plane of polarization parallel and perpendicular to the fiber axis, using an Aus Jena Interference microscope. The birefringence reported for a fiber is obtained as the average from a set of 10 measurements on individual filaments. The refractive index of the immersion liquid used was 1.5.

Stress−strain curves of the fiber samples were obtained using an Instron tensile tester, Model 1125. Gauge lengths of 5 in. (127 mm) and nominal strain rates of ~7 and 0.07 min^{-1} were employed. Average strength, elongation at break, and work of rupture (strain energy at failure) were determined from the stress−strain curves of 10 samples. A Polymer Laboratories Minimat Tensile Tester was used to obtain the stress−strain behavior at various temperatures from 28 °C to 100 °C. The fiber bundle was glued to a 1-cm cardboard tab. The webs of the tab were cut after the sample had been positioned between the clamps.

Dynamic mechanical thermal analyses were conducted at 1 and 10 Hz using a Seiko Instruments Model DMS 210 operating in the tension mode. An initial tensile force of 0.2 N was applied to the fiber bundle clamped at two ends at an initial length of 10 mm. The tensile force was gradually diminished as the temperature was increased at 2 °C/min from −100 to +200 °C to compensate for the reduction in tensile modulus. A thin ceramic paper was placed between the sample and the clamps to avoid direct contact of the fiber with the sharp edges of the metallic clamps in this instrument.

A Seiko Instruments TMA/SS120C thermomechanical analyzer was used to perform nonisothermal deformation analysis (change in length as a function of temperature). The fiber bundle (initial length 5 mm) was subjected to a fixed load, and the temperature was increased at a rate of 10 °C/min. These experiments were performed at constant loads corresponding to initial stresses in the range 0.5−20 MPa.

Torsional moduli were estimated using a torsion pendulum in a vacuum chamber at a pressure of 5 in. (12.7 cm) of mercury. A single filament was glued to a cardboard tab that was attached to the inertia disk, a small flat circular cardboard disk, by means of an adhesive tape of constant dimensions; the webs of the tab were cut so as to have identical tab pieces on the bottom end for each fiber specimen. The procedures for measuring the period of oscillation and for computing the torsional shear modulus, with due account of viscous dissipation and aerodynamic drag, are described in the literature.[17,18]

Table 1. Properties of Poly(4-methyl-1-pentene) Fibers Measured at Room Temperature before and after Heat Treatment at 100 °C for 2 min

PMP fibers	tensile modulus (MPa)[a]	tenacity (MPa)[a]	breaking strain	crystal orientation function
as-spun				
pristine	1949	235	0.30	0.91
heat-treated, constrained	1957	235	0.30	0.92
heat-treated, unconstrained	1952	232	0.30	0.92
drawn (draw ratio = 1.5)				
pristine	2030	242	0.28	0.91
heat-treated, constrained	2041	245	0.28	0.91
heat-treated, unconstrained	2030	240	0.29	0.89

[a] Assuming a constant density of 0.83 g/cm^3.

Wide-angle X-ray diffraction measurements were conducted using a Rigaku-Rotaflex RU-200 rotating anode generator, operating at 100 mA and 45 kV, with a horizontal θ-2θ diffractometer. Nickel-filtered copper Kα radiation (wavelength 0.154 nm) was used for all measurements. Azimuthal scans were performed on the (200) reflection to compute the Hermans orientation function, f_c, using the Wilchinsky method.[19] WAXD flat plate photographs of the samples, each wound as a parallel array of filaments on the temperature-controlled sample holder, were obtained with a Statton camera. A sample-to-film distance of 5.5 cm, an exposure time of 2 h, and a point collimation of 0.38 mm were used.

For the solid-state NMR experiments, as-received PMP pellets (melt index = 8, Aldrich Chemical Co.) were melt-pressed into a cylindrical form (5.5-mm diameter) to fit into the ceramic sample rotors. NMR spectra were taken on a Bruker MSL 300 spectrometer (7 T) under magic-angle spinning (MAS) at 4 kHz using recycle delays of 2 s. Proton and carbon 90° pulses of 3.8−4.2 μs were used. The ^{13}C CP/MAS spectra were measured with a cross-polarization time of 1 ms. The 2D Wideline Separation (WISE) spectra[20,21] were acquired with either a 100-μs or 1-ms cross-polarization time. The spectral width in the ^1H (t_1) dimension was 200 kHz: a dwell time of 5 μs was incremented at least 64 times. Dwell times of 40 μs in the ^{13}C (t_2) dimension were employed.

Results and Discussion

Initial Properties and Structure. Table 1 shows the tensile modulus, breaking strength, and breaking strain of as-spun and drawn fibers of PMP at room temperature. The modulus is computed as the initial slope of the stress−strain curve. The cross-sectional area of the as-spun fiber bundle was determined to be 0.03 mm^2 from bulk and linear density measurements. This value was also confirmed by optical microscopy. It is evident from these data that the change in mechanical properties upon drawing to a draw ratio of 1.5 is essentially negligible.

Calorimetric thermograms (DSC scans) for both drawn and as-spun fibers were found to be very similar. Table 2 summarizes the DSC data. The crystallinity in these fibers, obtained from the enthalpy of melting, is found to be as high as 75%. No evidence for additional crystallization was seen in the thermograms obtained during heating to the melt. As observed previously for PMP,[22,23] and often for semicrystalline polymers in

Table 2. Calorimetric Data Obtained for As-Spun and Drawn (Draw Ratio = 1.5) Poly(4-methyl-1-pentene) Fibers

property	as-spun	drawn
melting temperature (°C)	238	238
heat of fusion (J/g)	46	47
crystallinity (%)	74	76
crystallization temperature (°C)	210	211
heat of crystallization (J/g)	46	45

general, differential scanning calorimetry does not provide unambiguous evidence for the presence of a glass transition.

The refractive index measured with polarization parallel or perpendicular to the fiber axis is found to be the same, 1.47, indicating the birefringence to be ~0. However, this does not imply that the material is isotropic, as one observes a high degree of orientation in the fibers from wide-angle X-ray diffraction azimuthal scans. The absence of any birefringence is a consequence of the structural similarity of the main chain and the pendant groups. The crystal orientation function, $f_{c,z}$, was determined to be ≈0.91 from the azimuthal scan of the (002) reflection ($2\theta = 9.3°$) for both as-spun and drawn fibers, indicating a very high degree of crystalline orientation.

It can be seen clearly from the above-mentioned observations that the PMP fibers in this study are well crystallized, with highly oriented crystals. Although it has not been established directly due to lack of intrinsic optical anisotropy in PMP, the fibers should also possess a significant anisotropy in the noncrystalline fraction as a consequence of melt spinning and drawing. The mechanical properties of PMP are only marginally improved by drawing, a result that has been well-known in industrial practice with this polymer.

Changes in Properties and Structure with Temperature. Figure 1A shows the typical changes in dynamic moduli, E' and E'', with temperature. A major peak in tan δ is obtained around 45 °C, but no evidence of other transitions at temperatures up to ~180 °C is seen for these fiber bundles. The storage and loss moduli exhibit a steady decline, beginning at ~40 °C. The storage modulus at 50 °C is only 27% of its original modulus observed below the transition temperature. Figure 1B shows that a similar trend is observed in the change of torsion modulus with temperature, that is, the torsion modulus at 50 °C is only about a third of its value at room temperature. The same trends are observed in both as-spun and drawn fibers.

Figure 2 shows the elongation vs temperature obtained at different stress levels in the nonisothermal deformation analysis. The temperature at which the slope of the elongation vs temperature curve tends to infinity is the "failure" temperature at that particular stress. This failure temperature falls rapidly with increase in stress levels (Figure 3).

Figure 4 shows the stress−strain curves at different temperatures for the drawn and as-spun fibers at two strain rates, 7 and 0.07 min^{-1}, that differ by 2 orders of magnitude. These data confirm that PMP indeed exhibits a pronounced drop in tenacity with increase in temperature. The breaking strength at 100 °C is about 5% of its strength at room temperature. By integration of the area under these stress−strain curves, the work of rupture may be obtained and is plotted in Figure 5 as a function of temperature for the two deformation rates (the computed curves will be described in the following section). The differences in these work-of-rupture curves for the two deformation rates is indicative of differences in viscous dissipation at these rates. Thus, while the viscous dissipation contribution to work of rupture is significant at room temperature, it diminishes to less than 10% at temperatures of 70 °C and above.

Table 1 provides a comparison of the mechanical properties and the crystalline orientations, measured at room temperature, before and after heat treatment at 100 °C for 2 min. The stress−strain curves are

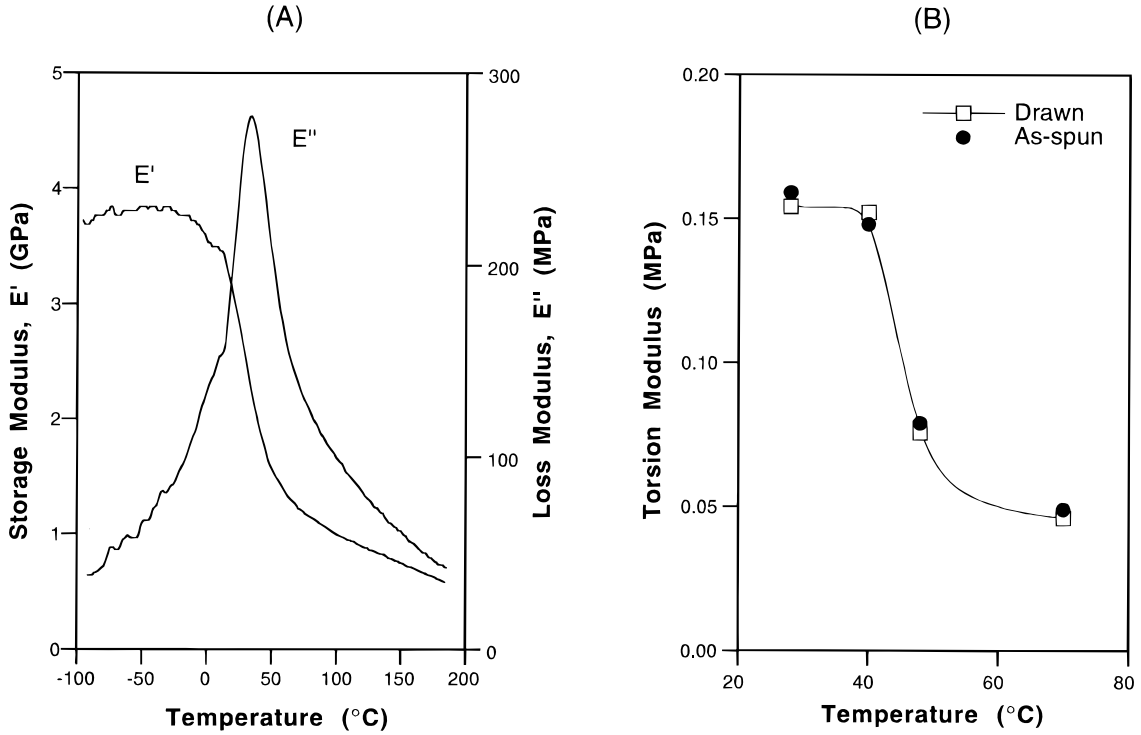

Figure 1. (A) Storage modulus (E') and loss modulus (E'') of drawn PMP fibers as a function of temperature. Testing frequency = 1 Hz. (B) Changes in torsion modulus of PMP fibers with temperature.

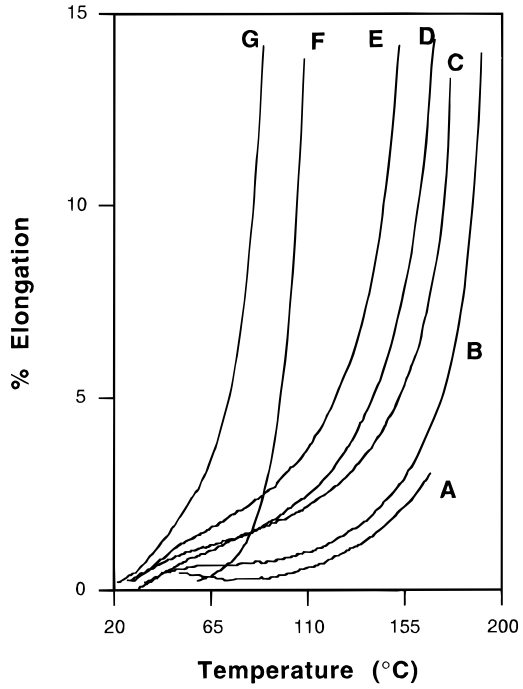

Figure 2. Deformation of drawn PMP fibers as a function of temperature for various initial stress levels: (A) 0.7 MPa; (B) 1.6 MPa; (C) 3.3 MPa; (D) 4.9 MPa; (E) 6.5 MPa; (F) 13 MPa; (G) 19.6 MPa. The temperature at which the slope tends to infinity is the "failure" temperature at that stress.

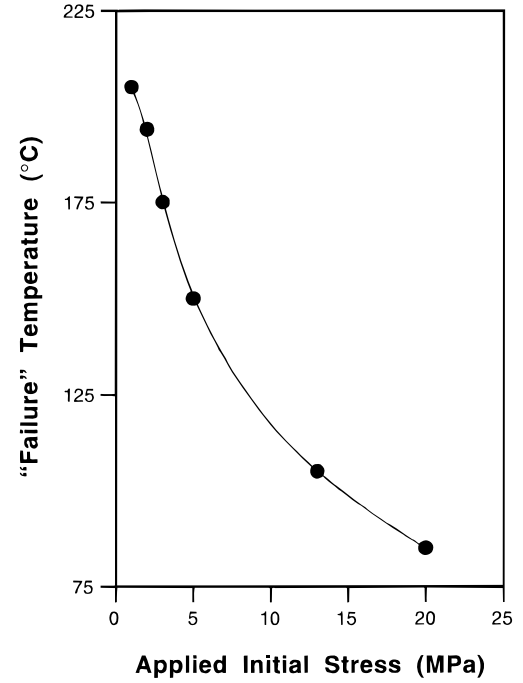

Figure 3. "Failure" temperature of drawn PMP fibers as a function of initial stress.

identical for the samples tested before and after annealing, irrespective of constrained or unconstrained annealing conditions. The crystalline orientation functions and the calorimetric thermograms also show no significant changes.

Since no apparent mechanisms for any reversible loss of order can be envisioned, it is unlikely that the loss of mechanical properties at these temperatures results from any disordering of the structure in the PMP fibers. It is also important to note that no thermorheological response that might indicate the onset of any such changes, especially pronounced thermal stress or thermal shrinkage, is observed when the fibers are heated from room temperature to 100 °C (Figure 2). These inferences are further corroborated by the wide-angle X-ray diffractograms obtained at different temperatures. The flat plate photographs (Figure 6) show that the crystal structure and the orientational order of crystals do not change even when the temperature is raised to as high as 130 °C.

Mechanism for Loss of Strength in PMP at Moderate Temperatures. The different observations can be summarized as follows:

i. PMP does lose a substantial fraction of its mechanical properties (tenacity, work of rupture) in tension when its temperature is raised above room temperature, especially above ~50 °C.

ii. No evidence is found for any significant disordering of the structure at the temperatures associated with this dramatic loss of strength. Also, the properties are virtually unchanged from those of the original material when the temperature is reduced back to room temperature.

iii. The large reduction in mechanical properties occurs with a major dynamic mechanical transition, reported to be the glass transition of PMP. This transition is clearly marked by a maximum in the loss modulus, E'', and a large decrease in both storage modulus, E', and torsional modulus of the PMP fibers. It should be noted, however, that this transition is not accompanied by thermorheological responses that are invariably associated with the glass transition in oriented semicrystalline polymers, such as the *pronounced* onset of thermal shrinkage or development of thermal stress.

iv. The viscous dissipation associated with tensile deformation diminishes significantly when the temperature is increased, vanishing almost completely, to less than 10% of work of rupture, at temperatures above 70 °C.

The final point provided the key to quantitative rationalization of the loss of work of rupture and strength in PMP. It is based on a *melting-dictated thermodynamic limit* to maximum reversible work of deformation in all uncross-linked crystalline materials that has been established by Abhiraman.[24] The premise here is that an upper limit to reversible work in uncross-linked crystalline materials is set by a deformation-dictated lowering of the equilibrium melting temperature to the deformation temperature, that is, raising of the free energy of the solid material to that of the melt at the deformation temperature. With the implied absence of dissipation and some minor approximations associated with differences in specific heats, the melting-dictated maximum reversible work, W_{max}^{rev}, is given by

$$W_{max}^{rev}(T) = \Delta H_m^*(1 - T/T_m^*) \qquad (1)$$

where $W_{max}^{rev}(T)$ is the melting-dictated upper bound to reversible work, that is, the reversible work of deformation that would lead to the equilibrium melting temperature being reduced to the test temperature, T. ΔH_m^* is the enthalpy of melting of unstrained PMP, and T_m^* is the equilibrium melting temperature of unstrained PMP.

The requirement of reversibility dictates that there should be no dissipation during deformation, a condition that is clearly approached in the deformation of PMP at higher temperatures (Figure 5). The predictions

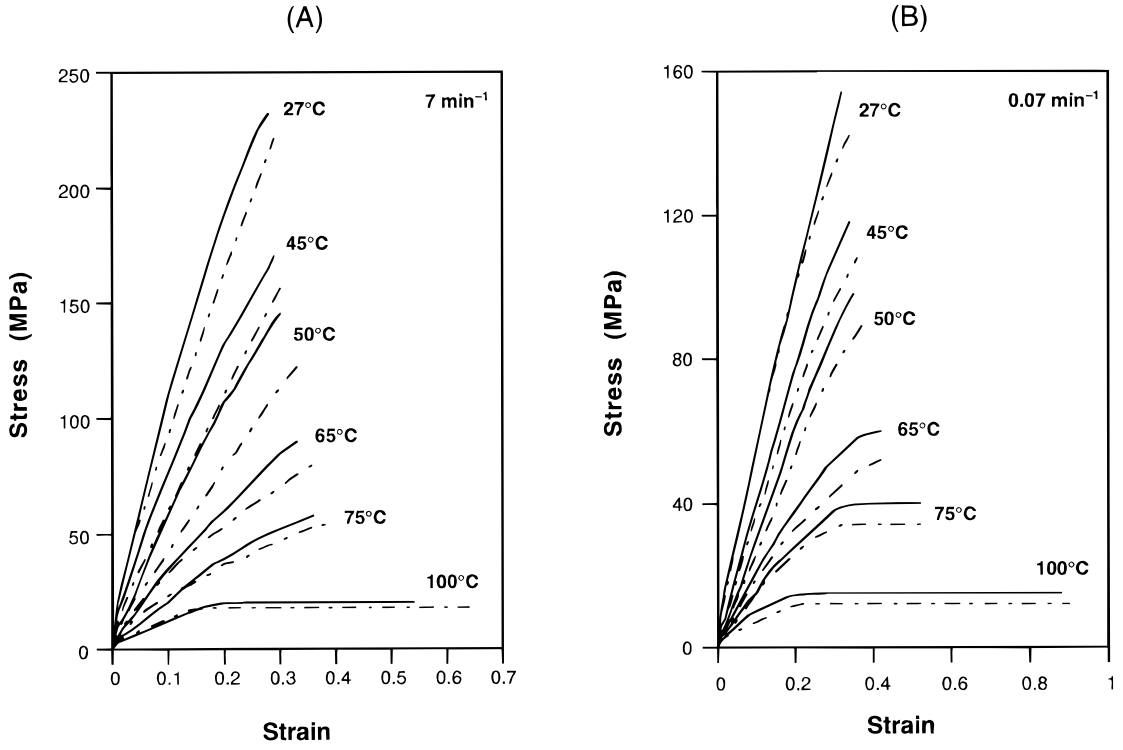

Figure 4. Stress-strain curves for as-spun and drawn PMP fibers at different temperatures: (A) strain rate = 7 min^{-1}; (B) strain rate = 0.07 min^{-1}. Key (—) drawn; (— • —) as-spun.

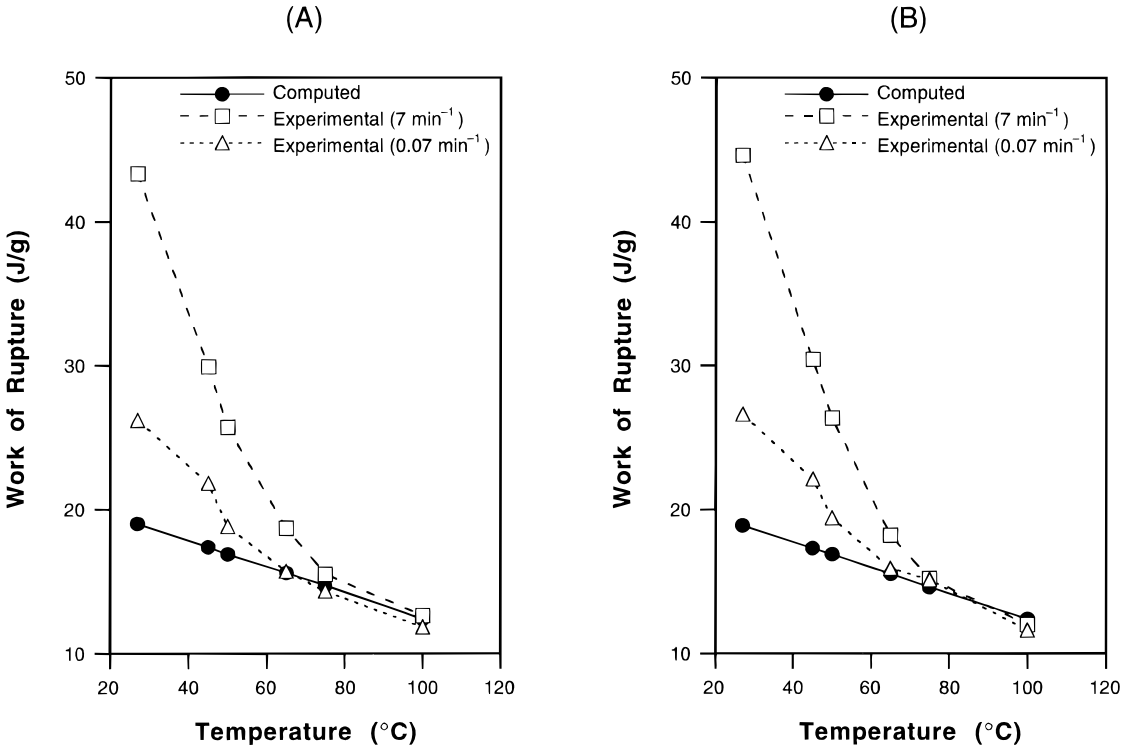

Figure 5. Comparison of predicted maximum reversible work of rupture and the experimental work of rupture (W_{exp}) at strain rates of 7 and 0.07 min^{-1}: (A) drawn fibers; (B) as-spun fibers. Excellent agreement is seen between the predicted and experimental responses under conditions of negligible dissipation, i.e., at the high-temperature portions of the curves where the work of rupture tends toward zero.

based on eq 1, with ΔH_m^* and T_m^* obtained experimentally from calorimetric analysis, are also shown in Figure 5 as the computed curves. There is a remarkable agreement between the thermodynamically predicted limit of reversible work and the experimentally observed work of rupture under conditions that have been seen to generate very little dissipation, that is, where it becomes essentially independent of the rate of deformation. An unfortunate implication of this finding is that the problem encountered in PMP with regard to its precipitous loss of tensile properties at temperatures well below its melting temperature is intrinsic to the material.

Molecular Mechanism for Disappearance of Viscous Dissipation in PMP. An important question that arises here pertains to the reason for the almost

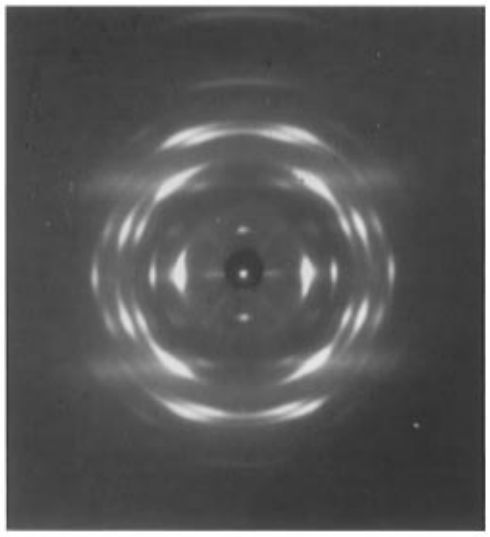

A

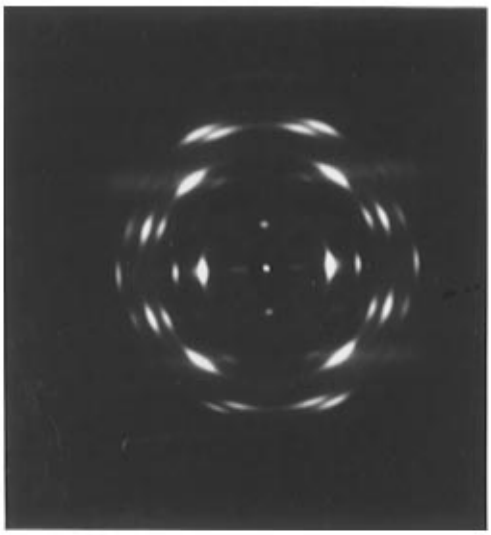

B

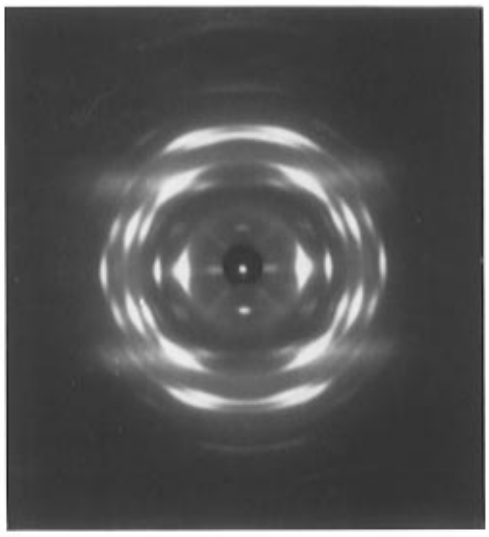

C

Figure 6. Flat-plate wide-angle X-ray diffraction photographs of drawn PMP fibers at different temperatures: (A) 30 °C; (B) 75 °C; (C) 130 °C. The crystalline structure remains essentially unchanged in this temperature range.

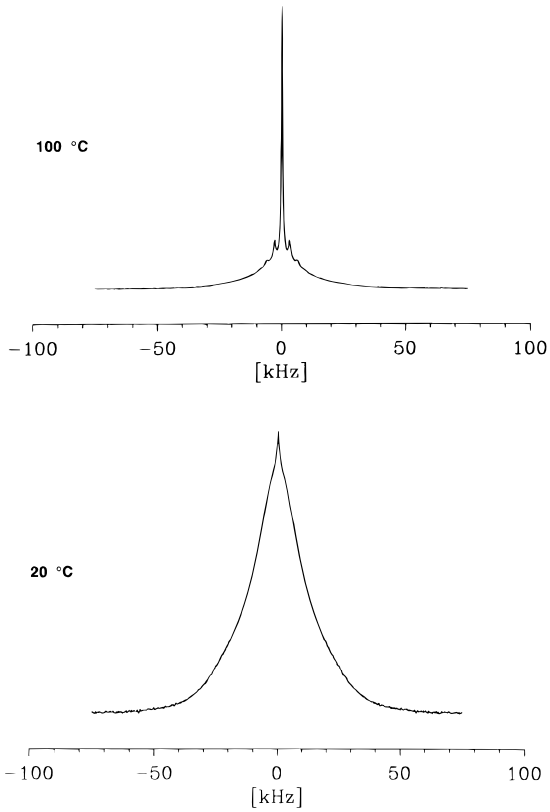

Figure 7. ^{1}H solid-state NMR spectra of PMP at 20 and 100 °C, recorded with MAS at 4 kHz.

complete elimination of viscous dissipation in tensile deformation of oriented PMP at temperatures above its 45 °C dynamic mechanical transition. Since thermorheological responses that would be characteristic manifestations of backbone motions in oriented polymers were absent, the initial inference was that it had to be related to pendant group motions.

Solid-state NMR was used to identify the mobile entities in the PMP molecular structure as the temperature is raised. Solid-state ^{1}H NMR spectra were first reported for this polymer in 1961; wideline spectra were measured as a function of temperature from −196 to +77 °C.[25,26] The ^{1}H line widths gradually decreased with increasing temperature and then dropped sharply at about 45 °C. At this temperature, the line shape develops a bicomponent structure consisting of a narrow component, characteristic of mobile moieties, superimposed on a broad component, characteristic of rigid moieties. The sharp drop at 45 °C was identified as the glass transition of PMP, and thus attributed to the side-chain *and* main-chain motions that accompany a typical glass transition in a semicrystalline polymer. The gradual decrease in the line width observed from −196 to 45 °C was attributed to side-chain motions.[26]

In Figure 7, solid-state ^{1}H wideline spectra are shown for PMP at 20 °C and 100 °C. Whereas the spectrum at 20 °C is dominated by a broad component indicative of a highly immobilized solid, the spectrum at 100 °C exhibits a dominant sharp line flanked by spinning sidebands. This indicates fast but anisotropic motion.[20] Since the ^{1}H spectra are completely dominated by the side group, which carries 9 out of 12 hydrogen atoms, this indicates rapid side-group motions subject to constraints imposed by a nonmobile backbone. In order to proceed further, the dynamics must be assigned to specific groups. However, structural information, as

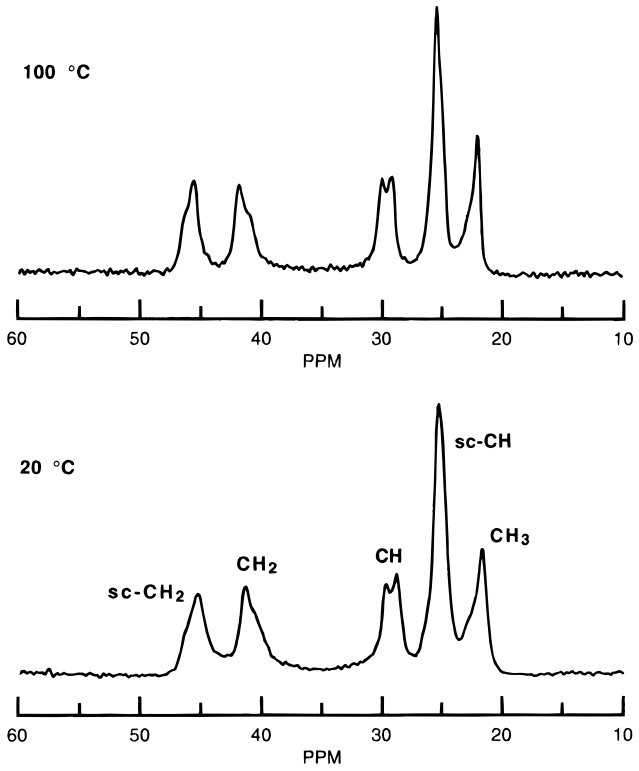

Figure 8. ^{13}C CP/MAS solid-state NMR spectra of PMP at 20 and 100 °C. Chemical shift values are given in the text; "sc" means "side-chain" (since CH_3's only exist in the side chains, these are not labeled with "sc").

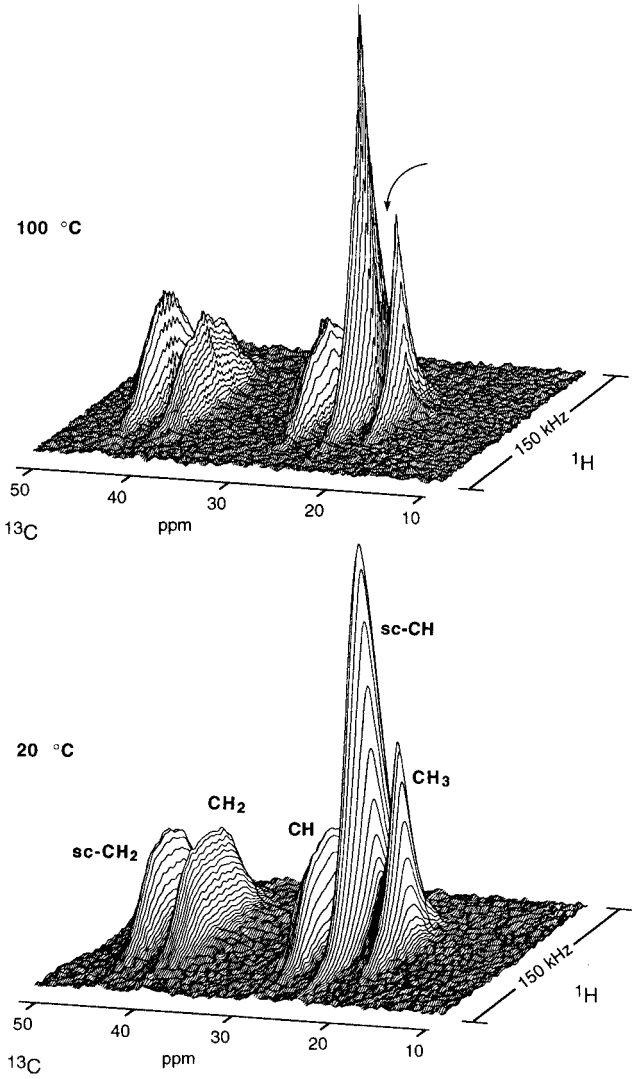

Figure 9. Two-dimensional WISE NMR spectra of PMP at 20 and 100 °C. The cross-polarization time is 100 μs. For the spectrum measured at 100 °C, a narrowed ^1H line shape is detected in the ^{13}C region between the side-group CH and CH_3's (indicated by an arrow).

embodied in the chemical shift, is unresolvable in ^1H widelines. The needed structural information is contained in the chemical shifts of the ^{13}C CP/MAS spectrum of PMP labeled in Figure 8. The peak assignments follow those of the high-resolution solution spectrum.[27] A single peak is present for every chemically distinct nucleus, with one exception: The backbone CH signal appears as a doublet due to solid-state packing effects. Shown for both 20 and 100 °C, the ^{13}C spectrum of PMP reveals absolutely no hint of the dynamical changes reflected in the ^1H wideline spectra at the same temperatures (Figure 7).

The dynamical information of ^1H wideline spectra can be combined and correlated with the structural information content of a ^{13}C NMR spectrum in a two-dimensional experiment in which the proton lines are separated in a second dimension according to their respective ^{13}C chemical shifts. This experiment, 2D *wi*deline *se*paration NMR (WISE NMR), has been used successfully for examining the structure and dynamics in various heterodynamic polymer systems.[28−30] The 2D WISE spectra for PMP are shown in Figure 9 at 20 °C and at 100 °C. For the spectrum measured at 20 °C, broad ^1H line shapes for all carbons of PMP are revealed. This indicates the absence of fast molecular motion in the tens of kilohertz regime. The same spectrum at 100 °C, measured 55 °C above the major dynamic mechanical transition, contains narrowed ^1H line shapes *only* for the terminal side-group carbons. This is seen along the ^{13}C dimension of the 2D WISE spectrum in the area between the side-group CH and CH_3's. It is marked by an arrow and more clearly seen in the 2D WISE spectrum of Figure 10, which was recorded with a longer cross-polarization time. WISE spectra generally discriminate against highly mobile components since the signal evolution depends on the transfer of magnetization via dipolar couplings from the ^1H's to the ^{13}C's. The cross-polarization time is the period in the experiment during which this transfer takes place; thus, increasing this period allows for more magnetization from the highly mobile ^1H's to transfer and appear in the 2D spectrum (dipolar couplings are much weaker for highly mobile segments). The only caveat is that the increased CP time also allows for spin diffusion to take place.[31] Spin diffusion occurs via successive spin flips of dipolar-coupled nuclei, and can lead to signal equilibration across the entire sample.[32] This is seen in Figure 10 where all the ^1H line shapes now appear triangular as a result of spin diffusion from the side-chain CH and CH_3's.

The appearance of the motionally-narrowed peak at a position shifted from the positions of the side-group CH (25.2 ppm) and CH_3's (21.7 ppm) is most likely the result of a difference in the conformation of mobile vs immobile side groups. Conformation effects can cause shifts of up to 4−5 ppm and are well-known in solid-state NMR.[33,34] The narrow component cannot be connected with the backbone carbons because its chemical shift (23.6 ppm) is too far removed from the backbone CH_2 (41.3 ppm) to be a conformationally shifted variation of this signal. While the backbone CH signal (doublet: 28.7, 29.8 ppm) is close enough, it is expected

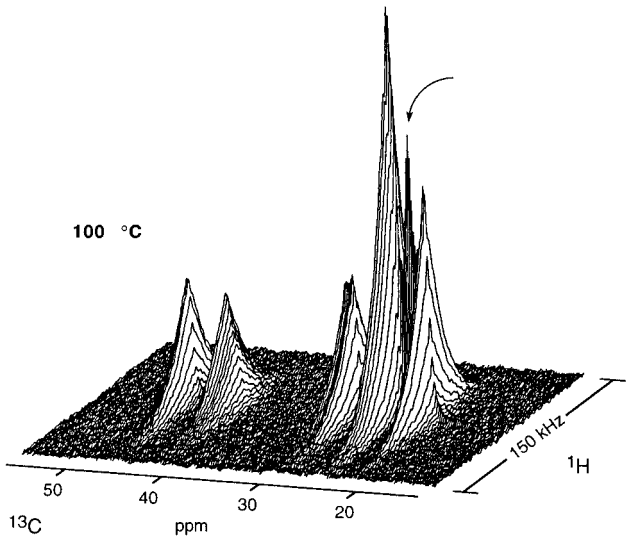

Figure 10. Two-dimensional WISE NMR spectrum of PMP at 100 °C measured with a longer cross-polarization time (1 ms) to allow for more magnetization transfer from highly mobile ^{1}H's. The arrow marks the highly mobile component.

that rapid motion of the backbone would result in the narrowing of both backbone carbon signals, and this is not observed. Since the side-chain CH_2 signal (45.3 ppm) remains broad, the motion must involve a rotation around the side-chain CH_2-CH bond.

Goldman−Shen experiments[35] at 100 °C (50-μs dephasing time) suggest the highly mobile side groups are primarily located within the more mobile regions of the material, most likely the noncrystalline or amorphous phase. According to Williams, Landel, and Ferry, the time scales of molecular motion in amorphous polymers should be shifted by more than 100 kHz from T_g to T_g + 50 °C,[36] which would lead to a narrowing of ^{1}H widelines. In semicrystalline systems, the restraints provided by crystallites would undoubtedly raise this temperature. Linear polyethylene exhibits a dynamic mechanical glass transition of about −110 to −100 °C.[37,38] ^{2}H NMR studies of ^{2}H-labeled polyethylene reveal that all noncrystalline methylenes exhibit restricted anisotropic mobility at −80 °C on a time scale of about 20 kHz.[39] For PMP, despite being 55 °C above the widely presumed T_g, motionally narrowed ^{1}H lines are not observed for the backbone motions on this time scale, but only for the side groups. No indications of fast main-chain motion have been found. Rotation of the pendant groups, combined with the very low density of packing of the main chains (moles of chains per unit cross-sectional area in PMP is $\sim^1/_2$ of that in polypropylene and ∼1/4 of that in polyethylene), generates a self-lubricated system manifested by negligible dissipation during deformation of this polymer.

Similar behavior has been reported for some copolyglutamates with alkyl side chains.[40] Described as "hairy rod" molecules, these polymers exhibit three dielectric-active relaxation processes, and a calorimetric T_g of −35 °C. Solid-state NMR studies show that the peptide backbone does not relax, but maintains its helical conformation at least up to 97 °C, the same temperature at which PMP exhibits fast motions for the side chains only. It is possible that the chain motions traditionally associated with glass transitions in semicrystalline polymers occur in PMP at temperatures higher than 45 °C. Using 2D ^{13}C exchange NMR, slow motions (time scales of milliseconds to seconds) were detected in PMP at 100 °C, although unambiguous assignments to specific structural units of the polymer were not possible. As discussed earlier, dynamic mechanical analyses have shown as many as four loss peaks between room temperature and 200 °C. A detailed analysis of these transitions, their associated molecular motions and thermorheological consequences is necessary before any definitive conclusions can be reached regarding the T_g of PMP.

The work presented here represents the merging of two originally independent studies: one on the morphology and temperature-dependent mechanical properties of PMP fibers and the other on temperature-dependent solid-state NMR spectroscopy of PMP moldings. Each was found to reinforce the inferences made from the other. While it would be most appropriate to have all the data from the same materials, the conclusions drawn here from the NMR studies pertain primarily to side-group motions, which are much less influenced by morphological differences than main-chain motions. Evidence of this was provided by acquiring the ^{1}H wideline spectra of the PMP fibers. The spectra, obtained at 20 and 100 °C, are identical to the corresponding spectra of the moldings shown in Figure 7.

Ultra-drawn PMP exhibits a room-temperature stress−strain behavior that is dramatically different from that of normally processed PMP.[41−43] The dissipative characteristics as well as the consequences of the 45 °C transition in the stress−strain behavior may also be different in ultra-drawn PMP. This highly crystalline PMP should be explored, especially with respect to any implications regarding molecular motions in the crystalline and noncrystalline phases.

Conclusions

It is clear that the performance limits of PMP are determined by thermodynamics of melting-dictated initiation of failure, with negligible contribution from viscous dissipation at temperatures above a major dynamic mechanical transition that occurs around 45 °C in this polymer. The molecular origin of this phenomenon has been found to be in the motions of the pendant group, especially rapid rotation about the side-chain CH_2-CH bond. Such rotation of the pendant group, combined with the very low density of packing of the chains, generates a self-lubricated system, causing negligible dissipation during deformation of this polymer. This finding requires revision of the previously held view that the transition around 45 °C in PMP denotes a classical glass transition accompanied by the onset of significant backbone segmental mobility. It also raises the prospects for research on fundamental mechanisms governing viscous dissipation during deformation of solid polymers.

Acknowledgment. The solid-state NMR work was funded in part by an NSF postdoctoral fellowship (H.W.B.). The Max-Planck Society provided fellowship support for A.S.K. The Polymer Program Associates of Georgia Institute of Technology provided a partial fellowship for S.R. Some assistance from Shalini Thadani, Ravi Kishore Sura, and Ying Liang of Georgia Tech is gratefully acknowledged. Discussions with Professor Ray Fornes (North Carolina State University) were of great help in postulating the molecular mechanism for the elimination of viscous dissipation in PMP.

References and Notes

(1) Kissin, Y. W. In *Encyclopedia of Polymer Science and Engineering*; Wiley-Interscience: New York, 1987; Vol. 9, p 707.
(2) Griffith, J. H.; Rånby, B. G. *J. Polym. Sci.* **1960**, *44*, 369.
(3) Litt, M. *J. Polym. Sci.: Part A* **1963**, *1*, 2219.
(4) Kusanagi, H.; Takase, M.; Chatani, Y.; Tadokoro, H. *J. Polym. Sci., Polym. Phys. Ed.* **1978**, *16*, 131.
(5) Lopez, L. C.; Wilkes, G. L.; Stricklen, P. M.; White, S. A. *J. Macromol. Sci., Rev. Macromol. Chem. Phys.* **1992**, *C32*, 301.
(6) Puleo, A. C.; Paul, D. R.; Wong, P. K. *Polymer* **1989**, *30*, 1357.
(7) Reddy, S. M.S. Thesis, Georgia Institute of Technology, 1992; p 10.
(8) Kirshenbaum, I.; Isaacson, R. B.; Feist, W. C. *Polym. Lett.* **1964**, *2*, 897.
(9) Crissman, J. M.; Sauer, J. A.; Woodward, A. E. *J. Polym. Sci.: Part A* **1964**, *2*, 5075.
(10) Woodward, A. E.; Sauer, J. A.; Wall, R. A. *J. Polym. Sci.* **1961**, *L*, 117.
(11) Takayanagi, M.; Kawasaki, N. *J. Macromol. Sci., Phys.* **1967**, *B1*, 741.
(12) Choy, C. L.; Luk, W. K.; Chen, F. C. *Polymer* **1981**, *22*, 543.
(13) Michel, P.; Dugas, J.; Cariou, J. M.; Martin, L. *J. Macromol. Sci., Phys.* **1986**, *B25*, 379.
(14) Rånby, B. G.; Chan, K. S.; Brumberger, H. *J. Polym. Sci.* **1962**, *58*, 545.
(15) Tanigami, T.; Yamaura, K.; Matsuzawa, S.; Miyasaka, K. *Polym. J.* **1986**, *18*, 35.
(16) Zoller, P.; Howard W. Starkweather, J.; Jones, G. A. *J. Polym. Sci.: Part B, Polym. Phys.* **1986**, *24*, 1451.
(17) Damodaran, S. Ph.D., Georgia Institute of Technology, 1991.
(18) Adams, R. D.; Lloyd, D. H. *J. Phys. E, Sci. Instrum., Ser. 2* **1975**, *8*, 475.
(19) Wilchinsky, Z. W. *J. Appl. Polym. Sci.* **1963**, *7*, 923.
(20) Schmidt-Rohr, K.; Clauss, J.; Spiess, H. W. *Macromolecules* **1992**, *25*, 3273.
(21) Schmidt-Rohr, K.; Spiess, H. W. *Multidimensional Solid-State NMR and Polymers*; Academic: New York, 1994.
(22) Melia, T. P.; Tyson, A. *Makromol. Chem.* **1967**, *109*, 87.
(23) Lebedev, B. V.; Smirnova, N. N.; Vasil'ev, V. G.; Kiparisova, E. G.; Kleiner, V. I. *Polym. Sci., Ser. A* **1994**, *36*, 1171.
(24) Abhiraman, A. S. *Proc. R. Soc. London A*, in press.
(25) Woodward, A. E.; Odajima, A.; Sauer, J. A. *J. Phys. Chem.* **1961**, *65*, 1384.
(26) Chan, K. S.; Rånby, G.; Brumberger, H.; Odajima, A. *J. Polym. Sci.* **1962**, *61*, S29.
(27) Ferraris, G.; Corno, C.; Priola, A.; Cesca, S. *Macromolecules* **1977**, *10*, 188.
(28) Beckham, H. W.; Spiess, H. W. *Macromol. Chem. Phys.* **1994**, *195*, 1471.
(29) Kulik, A. S.; Haverkamp, J. *Polymer* **1995**, *36*, 427.
(30) Clauss, J.; Schmidt-Rohr, K.; Adam, A.; Boeffel, C.; Spiess, H. W. *Macromolecules* **1992**, *25*, 5208.
(31) Abragam, A. *Principles of Nuclear Magnetism*; Clarendon: Oxford, England, 1961.
(32) Clauss, J.; Schmidt-Rohr, K.; Spiess, H. W. *Acta Polym.* **1993**, *44*, 1.
(33) Earl, W. L.; VanderHart, D. L. *Macromolecules* **1979**, *12*, 762.
(34) Tonelli, A. *NMR Spectroscopy and Polymer Microstructure*; VCH: New York, 1989.
(35) Goldman, M.; Shen, L. *Phys. Rev.* **1966**, *144*, 321.
(36) Williams, M. L.; Landel, R. F.; Ferry, J. D. *J. Am. Chem. Soc.* **1955**, *77*, 3701.
(37) Kline, D. E.; Sauer, J. A.; Woodward, A. E. *J. Polym. Sci.* **1956**, *22*, 455.
(38) Wilbourn, A. H. *Trans. Faraday Soc.* **1958**, *54*, 717.
(39) Hentschel, D.; Sillescu, H.; Spiess, H. W. *Polymer* **1984**, *25*, 1078.
(40) Schmidt, A.; Lehmann, S.; Georgelin, M.; Katana, G.; Mathauer, K.; Kremer, F.; Schmidt-Rohr, K.; Boeffel, C.; Wegner, G.; Knoll, W. *Macromolecules* **1995**, *28*, 5487.
(41) Kanamoto, T.; Ohtsu, O. *Polym. J.* **1988**, *20*, 179.
(42) He, T.; Porter, R. S. *Polymer* **1987**, *28*, 946.
(43) He, T.; Porter, R. S. *Polymer* **1987**, *28*, 1321.

MA961139Q